RAPID COMMUNICATIONS

PHYSICAL REVIEW B VOLUME 51, NUMBER 14 1 APRIL 1995-II

Equivalent phenomena for commensurate vortex states and zero field in a modulated sine-Gordon system

M. A. Itzler and M. Tinkham

Department of Physics and Division of Applied Sciences, Harvard University, Cambridge, Massachusetts 02138

(Received 6 February 1995)

The presence of periodic columnar defects in large Josephson junctions leads to striking commensurability effects when a magnetic field is applied parallel to the defects. Through the measurement of dynamic and static phenomena involving fluxons in the junction, we confirm recent theoretical predictions that the properties of junctions with periodic defects at commensurate fields are identical to those of defect-free junctions at zero field if the critical current density j_c and penetration depth λ_J are rescaled to obtain field-dependent effective parameters $\tilde{j}_c$ and $\tilde{\lambda}_J$. We demonstrate the role of these effective parameters in describing the structure of current-voltage characteristics at commensurate fields and of the field-dependent critical current $I_c(H)$.

With the advent of high-temperature superconductivity, there has been a resurgence of interest in the properties of magnetic fluxons in superconductors. Since flux motion induces dissipation, the pinning of fluxons is of particular importance for the application of high-T_c materials. To this end, there is much to be learned by studying systems in which pinning is well controlled.

In a previous work,[1] we described flux pinning effects in large Josephson junctions with artificial defects created in the barrier using lithographic techniques. The effect of the defects on the inherently nonlinear behavior of large junctions[2] has already attracted considerable interest.[3] Such devices may also serve as models for testing some of the numerous theoretical predictions concerning flux pinning in 1+1 dimensions.[4–6]

Recently, Balents and Simon (BS) predicted[7] that in large Josephson junctions with periodic defects, the presence of a one-dimensional fluxon lattice commensurate with the defects leads to behavior equivalent to that of a defect-free junction near zero field. They demonstrate this by transforming a "modulated" sine-Gordon equation which describes the commensurate situation into the usual sine-Gordon equation for a uniform junction near zero field. From this mapping, they obtain field-dependent *effective* critical current densities $\tilde{j}_c$ and penetration depths $\tilde{\lambda}_J$ which govern the junction properties near commensurate fields. In this paper, we report detailed confirmation of predictions arising from the BS mapping.

Josephson tunnel junctions are formed by two superconducting electrodes coupled through an insulating barrier. The junction carries a supercurrent density

$$j(\mathbf{r}) = j_c(\mathbf{r})\sin\gamma(\mathbf{r}), \tag{1}$$

where $j_c(\mathbf{r})$ is the critical current density, $\gamma(\mathbf{r})$ is the gauge-invariant phase difference across the barrier, and $\mathbf{r}\equiv(x,y)$ is in the barrier plane. A magnetic field in the barrier induces phase winding:

$$\frac{\partial\gamma}{\partial x} = \frac{2\pi\Lambda}{\Phi_0}B_y, \quad \frac{\partial\gamma}{\partial y} = -\frac{2\pi\Lambda}{\Phi_0}B_x, \tag{2}$$

where $\Phi_0 = hc/2e$ is the flux quantum, and the magnetic thickness $\Lambda = 2\lambda + d$ (λ is the electrode penetration depth and d is the barrier thickness). The behavior of γ is given[8] by the modified sine-Gordon equation:

$$\frac{\partial^2\gamma}{\partial x^2} + \frac{\partial^2\gamma}{\partial y^2} - \frac{1}{\bar{c}^2}\frac{\partial^2\gamma}{\partial t^2} - \frac{\beta}{\bar{c}^2}\frac{\partial\gamma}{\partial t} = \frac{1}{\lambda_J^2}\sin\gamma, \tag{3}$$

where $\beta = \sigma_0/C$ arises from the quasiparticle conductance σ_0 and capacitance C per unit area of the junction. The fluxon velocity $\bar{c} = c/\sqrt{2\pi C\Lambda}$, and the Josephson penetration depth $\lambda_J = \sqrt{(c\Phi_0)/(8\pi^2\Lambda j_c)}$.

If $\mathbf{B}\|\hat{\mathbf{y}}$, then $\partial\gamma/\partial y = 0$ [Eq. (2)]. To find time-independent solutions of Eq. (3), we then solve

$$\lambda_J^2\frac{\partial^2\gamma(x)}{\partial x^2} = \sin\gamma(x). \tag{4}$$

Referred to as the stationary sine-Gordon equation, Eq. (4) has solutions[9] consisting of Jacobian elliptic functions.[10] For a field applied perpendicular to the junction width W [see Fig. 1(a)], strong screening ($\lambda_J \ll W$) results in localized 2π phase windings (solitons) corresponding to isolated Josephson fluxons of width $\sim 2\lambda_J$. For weak screening ($\lambda_J \gg W$), a uniform winding ($\gamma \propto x$) gives a sinusoidal current [Eq. (1)] and a constant field [Eq. (2)] in the junction.

In our junctions with periodic columnar defects, the critical current density $j_c(\mathbf{r})$ is reduced to zero at the defects; otherwise, $j_c(\mathbf{r}) = j_{c,\mathrm{bare}}$. If defects are oriented along $L\|\hat{\mathbf{y}}$, then $j_c(\mathbf{r}) \to j_c(x)$, and we can define a critical current per unit width $i_c(x) \equiv L j_c(x)$. Outside the defects, $i_{c,\mathrm{bare}} \equiv L j_{c,\mathrm{bare}}$. Equation (4) may then be generalized to a "modulated" sine-Gordon (SG) equation:

$$\lambda_J^2(x)\frac{\partial^2\gamma(x)}{\partial x^2} = \alpha(x)\sin\gamma(x) = i(x). \tag{5}$$

The function $\alpha(x) = i_c(x)/i_{c,\mathrm{bare}}$ vanishes where defects are present and is unity elsewhere.

In a recent paper,[1] we presented a model based on the premise that since $i_c(x) = 0$ wherever defects are present, Josephson currents are prevented from crossing the junction

0163-1829/95/51(14)/9411(4)/$06.00

© 1995 The American Physical Society

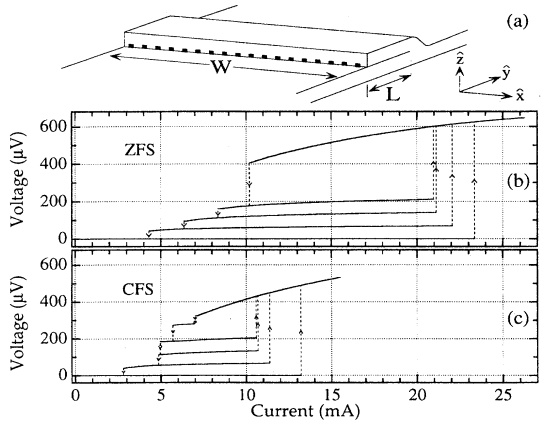

FIG. 1. (a) Overlap junction of width W with columnar defects embedded in barrier extending across length L. I-V characteristics exhibit (b) zero field steps (ZFS) at $H=0$ and (c) $n=1$ commensurate field steps (CFS) at $H=12.0$ Oe.

there. In the simplest version of the model, we assume a linear $\gamma(x)$. For a uniform junction, this gives a sinusoidal $i(x)$ with every positive half-wavelength balanced by a negative half-wavelength leaving no net current crossing the junction.[11] However, if periodic defects are present and $i(x)=\alpha(x)\sin\gamma(x)$ is commensurate with the defects, then each defect can block negative current, leaving net positive current crossing the junction. We used this "current blocking" model to compute[12] the critical current $I_c(n)$ for commensurate fields of n fluxons per defect by maximizing the total current

$$I=L\int_{-W/2}^{W/2} i_c(x)\sin[\gamma(x)+\gamma_0]dx \tag{6}$$

with respect to γ_0. If we coarse grain by averaging over the microscopic current configuration, we obtain an *effective uniform* critical current density $\tilde{j}_c(n)=I_c(n)/LW$ given by

$$\frac{\tilde{j}_c(n)}{j_{c,\mathrm{bare}}}=\begin{cases}\dfrac{\left|\sin n\pi\,\dfrac{w_d}{a}\right|}{n\pi}, & n>0,\\[2ex] 1-\dfrac{w_d}{a}, & n=0,\end{cases} \tag{7}$$

where w_d and a are the defect width and spacing. Since $\lambda_J\propto\sqrt{1/j_c}$, $\tilde{j}_c(n)$ has an associated *effective* penetration depth $\tilde{\lambda}_J(n)$ given by

$$\tilde{\lambda}_J(n)/\lambda_{J,\mathrm{bare}}=\sqrt{j_{c,\mathrm{bare}}/\tilde{j}_c(n)}. \tag{8}$$

Balents and Simon (BS) recently introduced[7] the effective parameters $\tilde{j}_c(n)$ and $\tilde{\lambda}_J(n)$ in a transformation of the modulated SG equation [Eq. (5)]. They change variables to $\eta(x)=\gamma(x)-(2\pi nx/a)$, which amounts to replacing H_y by an effective field $\tilde{H}_y=H_y-(n\Phi_0/\Lambda a)$. They also express the critical current profile $\alpha(x)$ in Eq. (5) as the Fourier sum $\Sigma_{m=0}^{\infty}\alpha_m\cos(2\pi mx/a)$. Assuming $a<\lambda_J$ and $\tilde{H}_y\Lambda\lambda_J\ll\Phi_0$ (which imply a fairly uniform field near a commensurate value), η will vary slowly on the scale of the defect spacing a, and the modulated SG equation [Eq. (5)] near a commensurate field reduces to $\tilde{\lambda}_J^2[\partial^2\eta(x)/\partial x^2]=\sin\eta(x)$, which is identical to Eq. (4) for a uniform junction with a small effective field $\tilde{H}_y$ and an effective λ_J:

$$\tilde{\lambda}_J(n)=\begin{cases}\sqrt{2/|a_n|}\,\lambda_J, & n>0,\\ \sqrt{1/\alpha_0}\;\lambda_J, & n=0.\end{cases} \tag{9}$$

Upon calculating the Fourier coefficients α_n, one obtains the same $\tilde{\lambda}_J(n)$ found using the current-blocking model [Eqs. (7) and (8)]. The BS transformation is also equally valid when applied to the *dynamic* SG equation [Eq. (3)] for a junction with defects since the time-dependent terms are unchanged.[7] Therefore, it predicts that the behavior of a junction with columnar defects near a commensurate field is *identical* to that of a junction without defects near zero field if $\tilde{j}_c(n)$ and $\tilde{\lambda}_J(n)$ replace $j_{c,\mathrm{bare}}$ and $\lambda_{J,\mathrm{bare}}$.

Dynamic Properties. To study dynamic properties of junctions with defects, we fabricated Nb/AlO_x/Nb junctions with $L=50$ μm and $W=200$ μm [Fig. 1(a)] in an overlap geometry (i.e., $L\sim\lambda_J\ll W$). Photolithographically defined, periodic SiO defects of width $w_d=2.9$ μm, spacing $a=10$ μm, and thickness $t_d\sim500$ Å extended over the 50 μm length. At 4.2 K, the zero-field critical current $I_c(0)\sim23.0$ mA yields $\tilde{j}_c(0)\sim300$ A/cm^2 and $\tilde{\lambda}_J(0)\sim24$ μm.

Since fluxon motion in the junction induces a voltage across it, dynamic properties can be probed by measuring I-V characteristics. With $H=0$, one finds the data shown in Fig. 1(b).[13] While sweeping I from zero, $V=0$ until $|I|>I_c(0)$. The sweep towards zero exhibits steps, and full plateaus are obtained by reversing the sweep direction while on a given step. These voltage plateaus at zero field, known as zero field steps (ZFS), result[14] from a solution of the SG equation [Eq. (3)] corresponding to the free propagation and edge reflection of current-induced fluxons. Each round trip excursion of a fluxon across the junction in a time $\Delta t=2W/\bar{c}$ induces a phase winding $\Delta\gamma=4\pi$ and a consequent voltage plateau at $V_p=(\Phi_0/2\pi)(\Delta\gamma/\Delta t)$. If m fluxons are present, a plateau is found at mV_p. For the plateaus in Fig. 1(b), the ~70 μV plateau spacing[15] yields a velocity $\bar{c}\sim c/40$, where c is the speed of light. By performing I-V measurements at the $n=1$ commensurate field (12.0 Oe), we obtained the data in Fig. 1(c). Again, we find plateaus with a ~70 μV spacing, as anticipated by the BS mapping since it does not change $\bar{c}$. We first reported these commensurate field steps (CFS) in Ref. 1.

The ZFS can be collapsed to a single curve if the voltage scale for a given plateau is rescaled by the number of fluxons m giving rise to it.[16] From the BS mapping, we expect an equivalent voltage scaling for the CFS. This is verified by Fig. 2(a), where the ZFS and CFS from Fig. 1 are plotted after rescaling each plateau by the appropriate m. However, the mapping yields an even stronger prediction that the dynamics at commensurate fields should be *identical* to zero field dynamics up to a rescaling of the *current density*. We carry out this final rescaling of the CFS *current* axis using the measured ratio $I_c(0)/I_c(1)=\tilde{j}_c(0)/\tilde{j}_c(1)=1.89$ to obtain the collapse of *all* the field steps to a single curve in Fig. 2(b).

Static properties. At the nth commensurate field, as I is swept from zero, the phase γ has static solutions with V

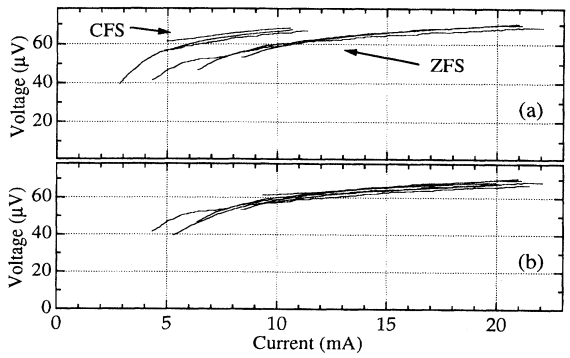

FIG. 2. (a) Collapse of ZFS and $n=1$ CFS after appropriate voltage rescaling of each step. (b) Collapse of all steps after CFS *current* axis rescaling by $\tilde{j}_c(0)/\tilde{j}_c(1)$.

$\propto \partial\gamma/\partial t=0$ until $|I|>I_c(n)$. To substantiate the predicted role of $\tilde{j}_c(n)$ and $\tilde{\lambda}_J(n)$ in determining the static properties of junctions with defects, we have studied large junctions for which $L,W\gg\tilde{\lambda}_J(n)$ over the range of field used. Sample dimensions were $L=1000$ μm and $W=200$ μm, and the SiO defects had width $w_d=2.8$ μm, spacing $a=10$ μm, and thickness $t_d\sim 500$ Å. We describe results for two samples with defects oriented as shown by insets in Figs. 3(a) and 3(b). $\tilde{\lambda}_J(0)\sim 50$ μm for both samples. I_c was determined using computer-controlled I sweeps and a 0.5 μV threshold.

Data taken on sample 1 are shown in Fig. 3(a). The zero field peak decays linearly with H due to the interference of the applied transport current with screening current $I_s\propto H$ induced to maintain zero field in the junction interior.[9] The

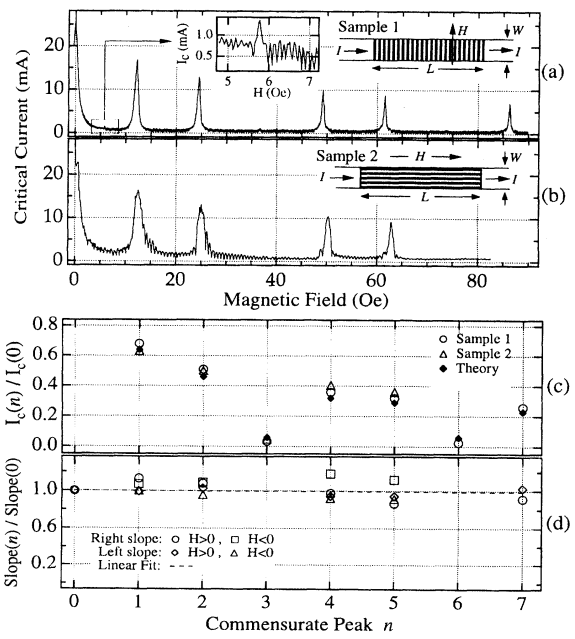

FIG. 3. $I_c(H)$ for (a) sample 1 and (b) sample 2 with insets showing defect orientation. Left-hand inset of (a) shows small peak near $\Phi_0/2$ per defect. (c) Normalized peak heights with prediction from text. (d) Collected slope data for sample 1; linear fit (dashed line) is constrained to unity at $n=0$.

extrapolation of this decay to zero defines a critical field $H_{c1J}=(2\Phi_0)/(\pi^2\Lambda\lambda_J)$ analogous to the lower critical field H_{c1} of type II superconductors.[8] We find similar peaks at commensurate fields with $n=$ 1, 2, 4, 5 and 7 flux quanta per defect. (The $n=3$ and $n=6$ peaks are suppressed because at these fields, each *defect* contains almost exactly an integral number of fluxons and will therefore always block nearly equal amounts of positive and negative current.[1]) The structure between the peaks arises from edge pinning.[11] In Fig. 3(b), data for sample 2 show peaks similar to those for sample 1, although their detailed shape is different mainly due to the change in the orientation of the screening currents relative to the transport current.

For junctions with $L\ll\lambda_J$, the critical current is $I_c=LWj_c$. If $L\gg\lambda_J$, then current crosses the junction only within a distance $\sim 2\lambda_J$ from each of the two edges where the electrodes overlap, and $I_c=4\lambda_J W j_c$ (the equality is exact[8]). Near commensurate fields in a junction with periodic defects, the relevant screening length is $\tilde{\lambda}_J(n)$. If $L\ll\tilde{\lambda}_J(n)$, the normalized peak heights are given by $I_c(n)/I_c(0)=\tilde{j}_c(n)/\tilde{j}_c(0)$. However, for peaks satisfying $L\gg\tilde{\lambda}_J(n)$, we must use *both* effective parameters to find

$$\frac{I_c(n)}{I_c(0)}=\frac{4\tilde{\lambda}_J(n)W\tilde{j}_c(n)}{4\tilde{\lambda}_J(0)W\tilde{j}_c(0)}=\sqrt{\frac{\tilde{j}_c(n)}{\tilde{j}_c(0)}}, \tag{10}$$

where Eq. (8) gives the second equality. In Fig. 3(c), the normalized peak height data for sample 1 (circles) and sample 2 (triangles) agree well with values (diamonds) predicted by Eq. (10).

The role of $\tilde{\lambda}_J(n)$ is also evident in the commensurate peak slopes determined by $I_c(n)/\tilde{H}_{c1J}(n)$ where $\tilde{H}_{c1J}(n)=[2\Phi_0]/[\pi^2\Lambda\tilde{\lambda}_J(n)]$ is an *effective* critical field for each commensurability peak. (Just as screening maintains zero field in the junction interior when H is near zero, it also maintains a commensurate field in the junction when H is near this field.) From Eq. (10), $I_c(n)\propto\tilde{j}_c(n)\tilde{\lambda}_J(n)$, $I_c(n)/\tilde{H}_{c1J}(n)\propto\tilde{j}_c(n)\tilde{\lambda}_J^2(n)$ is a constant [Eq. (8)], and so the peak slopes should be independent of n. (For $L\ll\tilde{\lambda}_J(n)$, slopes should be proportional to $[\tilde{j}_c(n)]^{1/2}$.) In Fig. 3(d), we show data from sample 1 for left-hand and right-hand slopes of the commensurate peaks normalized by the corresponding slope from the zero field peak; data are included for $H>0$ and $H<0$. A least-squares linear fit (dashed line) with the $n=0$ point constrained to unity shows that the normalized slopes are on average independent of n, as predicted.

The BS mapping assumes $\tilde{H}_y$ is small (i.e., H is nearly commensurate), but it is not easy to theoretically estimate the range of its validity. We previously reported[1] I-V curves taken as the field is changed from a commensurate value and demonstrated that their evolution is equivalent to that found near zero field for changes at least as large as $\tilde{H}_{c1J}(n)$. This suggests the mapping is valid for at least the field range beneath each peak.

Thus far, we have assumed a uniform H and phase winding $\gamma(x)=(kx+\gamma_0)$, where $k=(2\pi\Lambda H)/\Phi_0$. However, to first order, $i(x)\propto\sin kx$ will induce a sinusoidal modulation of H yielding $\gamma(x)=(kx+b\sin kx+\gamma_0)$, where b reflects the modulation strength and can be determined using measured parameters for the Jacobian elliptic solution for $\gamma(x)$ (for

sample 1, $b \sim 0.008$). Expanding $\sin(kx + b\sin kx + \gamma_0)$, we can generalize Eq. (6) to nonintegral fields:

$$\tilde{j}_c(H) = \int_{-W/2}^{W/2} dx \, \frac{i_{c,\mathrm{bare}}}{L} \sum_m \alpha_m \cos\frac{2\pi m x}{a} \left(\sin(kx + \gamma_0) + \frac{b}{2}\sin(2kx + \gamma_0) + O(b^2) \right), \quad (11)$$

where we have Fourier expanded $i_c(x) = i_{c,\mathrm{bare}}\alpha(x)$. Maximizing Eq. (11) for $H = \Phi_0/2\Lambda a$ (i.e., $\Phi_0/2$ per defect) gives $\alpha_1 b/2$, indicating finite subharmonic structure arising from the term of order b. (Structure at other fractional fields p/q scales with b^{q-1}.) We must consider that since $\tilde{\lambda}_J(1/2) \propto [\tilde{j}_c(1/2)]^{-1/2}$ exceeds the sample length L, we should use L instead of $\tilde{\lambda}_J(1/2)$ in computing $I_c(1/2)$[see Eq. (10) and preceding discussion]. Using the measured value of $I_c(0) = 26.1$ mA, we estimate $I_c(1/2) \sim 0.2$ mA, which is of the order of the small peak near $H = 6.0$ Oe [left inset of Fig. 3(a)].

The various phenomena we have presented may also occur for *nonperiodic* defect configurations. In the limit of an infinite sample, it is apparent from Eq. (11) [where a periodic $\alpha(x)$ had wave vectors $q = 2\pi m/a$] that $I_c(H)$ will be enhanced at any field $H = (q\Phi_0)/(2\pi\Lambda)$ for which the Fourier component α_q has finite weight, and it is plausible that commensurate field dynamic behavior would be found as well. We also expect that effects similar to those reported here should occur in any system described by the SG equation [Eq. (3)] with a modulated potential. Possible candidates include materials which exhibit commensurate charge density waves.

In summary, we have confirmed the theoretical prediction that the properties of large Josephson junctions with periodic defects near commensurate fields are identical to those of defect-free junctions near zero field up to the replacement of j_c and λ_J by field-dependent effective parameters $\tilde{j}_c(n)$ and $\tilde{\lambda}_J(n)$. This was demonstrated by dynamic measurements of ZFS and CFS, all of which can be collapsed to a single curve after a rescaling dictated by the theory. The static behavior probed through measurements of $I_c(H)$ shows that if *both* effective parameters are considered, normalized commensurate peak heights and slopes can be accurately calculated. In particular, these findings verify the predicted role of an effective penetration depth in governing junction screening properties when periodic defects are present.

We are grateful to Leon Balents and Steve Simon for helpful discussions and theoretical results prior to publication, and we thank Charles Owens for assistance with sample fabrication. This research was supported in part under the MRSEC program of the NSF under Contract No. DMR 94-00396, and by NSF Grant No. DMR-92-07956 and ONR Grant No. N00014-89-5-1565.

[1] M. A. Itzler and and M. Tinkham, Phys. Rev. B **51**, 435 (1995).

[2] *Nonlinear Superconductive Electronics and Josephson Devices*, edited by G. Costabile *et al.* (Plenum, New York, 1991).

[3] For a review, see A. V. Ustinov, in *Nonlinear Superconductive Electronics and Josephson Devices* (Ref. 2), p. 315.

[4] R. Fehrenbacher, V. B. Geshkenbein, and G. Blatter, Phys. Rev. B **45**, 5450 (1992); V. M. Vinokur and A. E. Koshelev, Zh. Eksp. Teor. Fiz. **97**, 976 (1990) [Sov. Phys. JETP **70**, 547 (1990)].

[5] M. P. A. Fisher, Phys. Rev. Lett. **62**, 1415 (1989); T. Hwa and D. S. Fisher, *ibid.* **72**, 2466 (1994).

[6] D. R. Nelson, Phys. Rev. Lett. **60**, 1973 (1988); T. Hwa, D. R. Nelson, and V. M. Vinokur, Phys. Rev. B **48**, 1167 (1993).

[7] Leon Balents and Steven H. Simon, Phys. Rev. B **51**, 6515 (1995).

[8] A. Barone and G. Paterno, *Physics and Applications of the Josephson Effect* (Wiley, New York, 1982).

[9] C. S. Owen and D. J. Scalapino, Phys. Rev. **164**, 538 (1967).

[10] M. Abramowitz and I. A. Stegun, *Handbook of Mathematical Functions* (Dover, New York, 1965).

[11] At a junction edge, it is possible to have as much as one uncompensated half-wavelength of Josephson current crossing the junction.

[12] The finite thickness t_d of the defects has been ignored but can be incorporated; see Ref. 1.

[13] Aside from the magnitude of $I_c(0)$, data are identical for junctions without defects at $H = 0$; see Ref. 1.

[14] K. K. Likharev, *Dynamics of Josephson Junctions and Circuits* (Gordon and Breach, Philadelphia, 1986).

[15] The decrease in plateau heights at lower currents is the result of damping effects which reduce $\tilde{c}$; see D. W. McLaughlin and A. C. Scott, Phys. Rev. A **18**, 1652 (1978).

[16] N. F. Pedersen and D. Welner, Phys. Rev. B **29**, 2551 (1984).